Fingering instability in nonadiabatic low-Lewis-number flames

Michael L. Frankel
Department of Mathematical Sciences, Indiana University–Purdue University at Indianapolis, Indianapolis, Indiana 46202-3216

Gregory I. Sivashinsky
The Levich Institute for Physico-Chemical Hydrodynamics, The City College of New York, New York, New York 10031
and School of Mathematical Sciences, Tel Aviv University, Ramat Aviv, Tel Aviv 69978, Israel
(Received 13 March 1995)

Employing the formal similarity between the dispersion relations for the hydrodynamic (Darrieus-Landau) and the diffusive instabilities at the quenching threshold, a phenomenological model for the nonlinear evolution of the near-limit premixed flame is proposed. Numerical simulations of the model show that at sufficiently high Zeldovich and low Lewis numbers the cellular flame resulting from the diffusive instability exhibits a tendency towards self-fragmentation resembling that known to occur in near-limit low-Lewis-number systems.

PACS number(s): 47.70.Fw, 82.40.Py

I. INTRODUCTION

A spherical flame spreading out from an ignition source is one of the most basic configurations of premixed combustion. While such flames are quite feasible in the laboratory, under certain conditions a nominally spherical flame becomes unstable and displays an irregular pattern of wrinkles. As is now well established, there are two principal mechanisms for the intrinsic flame instability: (i) thermal expansion of the burnt gas and (ii) high mobility of the deficient reactant (e.g., Sivashinsky [1]). The first, the so-called hydrodynamic or Darrieus-Landau mode of instability, is an invariable feature of any exothermic premixed gas flame. On the other hand, the occurrence of the second, the diffusive mode of instability, clearly depends on the composition of the mixture.

The outward propagating spherical flame in the regime of well-developed hydrodynamic instability appears as a multiple-scale fractal-like pebbly structure (e.g., Filyand, Sivashinsky, and Frankel [2]). To observe such a configuration the aspect ratio of the system should be rather large. For conventional hydrocarbon-air mixtures under normal pressure this would require the flame to be of several meters in diameter. In relatively small scale systems the hydrodynamically unstable flames are either completely smooth or exhibit a few wide-spaced ridges that are well maintained even under the deformation and extension of the flame. Unlike the former, the diffusive mode of instability manifests itself in the emergence of the small-scale irregularly recombining cellular structure and therefore is relatively easily produced under normal laboratory conditions. In sufficiently reactive, moderately nonadiabatic mixtures the cell in outward propagating flames does not increase in size once formed. When the spacing between cells promoted by the overall flame expansion exceeds a critical distance the cell splits up into new cells to keep the flame interface continuous.

However, for mixtures with sufficiently low reactivity, cells formed shortly after ignition do not sprout new cells; instead the expanding flame undergoes self-fragmentation. In some circumstances the fragments close up upon themselves to form stationary ball-like structures (Ronney [3]).

In real situations the hydrodynamic and diffusive instabilities may well coexist. Yet, in theoretical studies they are often analyzed separately, which is quite justified considering their distinction both in the physical origin and the scales involved. Hydrodynamic instability, thus, is considered mainly for relatively high-Lewis-number mixtures where the diffusive instability does not occur. Similarly, the diffusive instability is studied for the constant density limit, thereby suppressing the instability due to the thermal expansion.

For a weakly perturbed planar adiabatic flame the pertinent dispersion relations read (see, e.g., Sivashinsky [1])

$$\sigma=\tfrac{1}{2}\gamma U_a|k|+(\alpha-1)D_{\rm th}k^2 \tag{1}$$

for hydrodynamic instability, and

$$\sigma=(\alpha-1)D_{\rm th}k^2-4l_{\rm th}^2D_{\rm th}k^4 \tag{2}$$

for diffusive instability.

Here σ is the instability rate, k is the perturbation wave number; $\alpha=\frac{1}{2}\beta(\mathrm{Le}^{-1}-1)$, where β and Le are Zeldovich and Lewis numbers, respectively; $\gamma=1-\rho_b/\rho_u$ is the thermal expansion coefficient, with ρ_u and ρ_b being the densities of the fresh mixture and burnt gas, respectively; $D_{\rm th}$ is the thermal diffusivity of the system; U_a is the speed of the planar adiabatic flame relative to the burnt gas; $l_{\rm th}=D_{\rm th}/U_a$ is the flame width.

The relations (1) and (2) are written in the limit of weak thermal expansion ($\gamma\ll1$) and high Zeldovich number ($\beta\gg1$) when the system is close to the diffusive stability threshold, i.e., $\alpha\simeq1$.

The geometrically invariant evolution equations for the flame interface dynamics associated with the dispersion relations (1) and (2) read (Frankel [4])

$$\mathbf{n}\cdot\frac{d\mathbf{r}}{dt}=-U_a+(\alpha-1)D_{\rm th}\mathcal{K}+\frac{1}{2}\gamma U_a\left[1+\frac{1}{\pi}\int_S\frac{(\mathbf{r}-\mathbf{s})\cdot\mathbf{n}}{|\mathbf{r}-\mathbf{s}|^2}dS\right] \quad (3)$$

for hydrodynamic instability, and (Frankel and Sivashinsky [5(a)])

$$\mathbf{n}\cdot\frac{d\mathbf{r}}{dt}=-U_a+(\alpha-1)D_{\rm th}\mathcal{K}+4l_{\rm th}^2D_{\rm th}\mathcal{K}_{ss} \quad (4)$$

for diffusive instability.

Here $\mathbf{r}$ and $\mathbf{s}$ are the points on the two-dimensional flame interface, $\mathbf{n}$ is the normal directed to the burnt gas at the point $\mathbf{r}$, $\mathcal{K}=-\nabla\cdot\mathbf{n}$ is the flame curvature, and $\mathcal{K}_{ss}$ is its second-order arc-length derivative. In the three-dimensional (3D) version of the above equations one should interpret $\mathcal{K}$ as the mean curvature of the surface and $\mathcal{K}_{ss}$ should be replaced by the action of the Laplace-Beltrami operator $\Delta_s\mathcal{K}$ (Frankel and Sivashinsky [5(b)]), whereas in the integral term the coefficient becomes $1/2\pi$ and the denominator of the integrand is $|\mathbf{r}-\mathbf{s}|^3$ (Frankel [4]).

Below we present some results of numerical simulation of the geometrically invariant equations (3) and (4).

II. NUMERICAL SIMULATION

Before we discuss the results of simulation of Eqs. (3) and (4) a few words are due with respect to the numerical method used in it. After experimenting with various approaches we found that the most efficient for our situation is the most straightforward one. Namely, the equations were left in their original invariant (geometrical) form, the derivatives with respect to the arc length were evaluated explicitly by weighted finite differences, and the integral term was evaluated by the trapezoid method. We also used a split time step separating the action of the integral and the differential part of the operator.

Since we had to deal with rather large curve lengths and a huge number of integrals for each time level, the step of integration along the curve was scaled appropriately for the distant (from a given position $\mathbf{r}_i$ on the curve) pieces of the curve. This is possible in view of the decay of the interaction inversely proportional to the distance. In a sense, it is similar to integration with respect to the angle without being concerned with overlapping, which certainly occurs due to extremely complex behavior of the front.

At the same time the discrete curve representation by a polygon was homogenized with respect to the arc length to preserve an approximate fixed and equal spacing after every time step via a polynomial interpolation. The effect of homogenization turned out to be negligibly small when compared with the action of either part of the operator especially for the appropriately small time step, which was required anyway by the explicit finite-difference scheme. We should also add the polynomials of different degrees and types used in the interpolation produced qualitatively identical results even for very large times.

The explicit finite-difference approximation combined with our hardware limitations (PC) did not allow us to use very fine grids. With the total length reaching, say, about 3000 units even a step of 1/10 required about 30 000 vertices at the end of the computation. A necessity to operate with several (about 30) arrays of such size pushes the PC to its limit during the actual computation as well as with regard to the graphical presentation of the results. We should remark that the exponential growths of the total length exhibited by the fingering solutions of Eq. (4) would create similar difficulties even with a supercomputer that does not allow a considerable increase in evolution time unless a massively parallel code is used.

We verified our algorithm using a half-step grid and an appropriate time step, and, independently, a finer time step for each particular case. The results were qualitatively consistent and even quantitatively so for moderate times. We also tested our scheme for a combination of Eqs. (3) and (4) modeling roughly both the hydrodynamic and the diffusive instability in flames, and it seemed to produce reliable results consistent with physical predictions whenever such verification was possible. Additional verification of reasonable reliability of the numerical scheme is provided by a consistent simulation of Eq. (4) in the range of parameters where it leads to self-intersections producing fractal-like exponentially stretching curves that tend to cover the plane everywhere densely (Frankel [17]). One should think that successful performance of even such a simple straightforward computational method as ours should be attributed exclusively to the benign mathematical nature of Eqs. (3) and (4).

We should finally remark, before presenting the results, that, although the numerical approach used in the current work is sufficiently reliable to pinpoint the major effects discussed below, a real quantitatively accurate simulation would require a more sophisticated numerical approach and hardware. It should be added, however, that numerical methods for surface dynamics equations of the above type are a relatively new field of computational mathematics and still represent somewhat of a challenge and a serious one in the case of surfaces in the 3D space. Our computational ambitions, however, do not go that far.

Figure 1 presents results of the numerical simulation of Eq. (3) for $\gamma=0.8$ with $(1-\alpha)D_{\rm th}/U_a$ and $(1-\alpha)D_{\rm th}/U_a^2$ used as units of length and time. In these scales γ remains the only parameter of the equation

$$\mathbf{n}\cdot\frac{d\mathbf{r}}{dt}=-1+\mathcal{K}+\frac{\gamma}{2}\left[1+\frac{1}{\pi}\int_S\frac{(\mathbf{r}-\mathbf{s})\cdot\mathbf{n}}{|\mathbf{r}-\mathbf{s}|^2}dS\right]. \quad (3')$$

For convenience we have additionally rescaled both time and spatial coordinates by the factor of 10. Thus the dimensions and the times of the front configurations in Fig. 1 are 1/10 of the real ones.

A regular smooth perturbation of a very small amplitude is imposed on a nearly circular initial front, which results in a rapid development of well-pronounced wrinkles and cusps. The front configuration develops a fractal-like structure involving larger scales as it expands with constantly increasing speed.

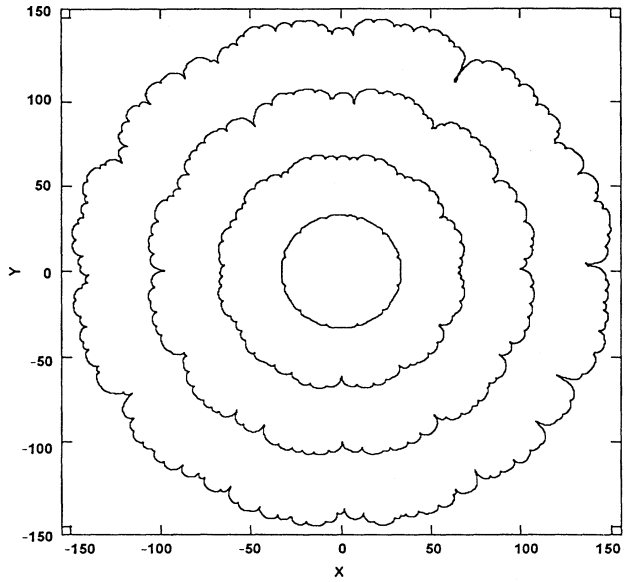

FIG. 1. Numerical simulation of Eq. (3) for hydrodynamically unstable flame ($\gamma=0.8$). Front configurations for $t/10=30$, 60, 90, 120; $\mathbf{r}/10=(X,Y)$.

Figure 2 depicts results of numerical simulation of Eq. (4) for $\alpha=1.3$ with $(\alpha-1)D_{\rm th}/U_a$ and $(\alpha-1)D_{\rm th}/U_a^2$ used as length and time scales. In these scales $\delta=4/(\alpha-1)$ remains the only parameter of the equation

$$\mathbf{n}\cdot\frac{d\mathbf{r}}{dt}=-1+\mathcal{K}+\delta\mathcal{K}_{ss}\ . \tag{4'}$$

Once again the dimensions and the times of the front

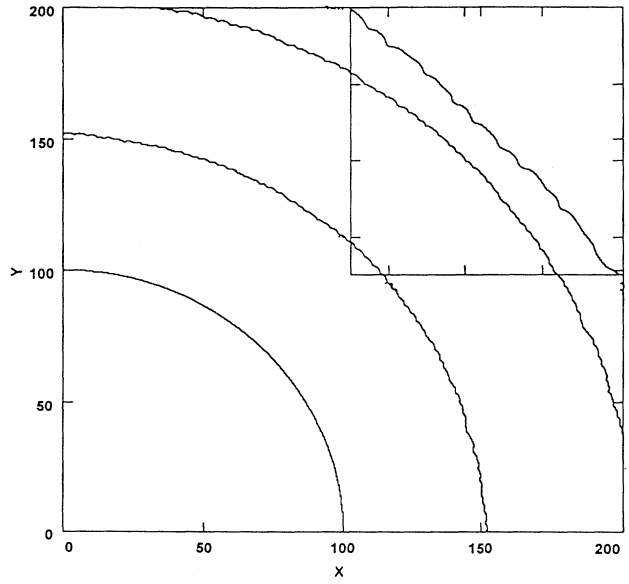

FIG. 2. Numerical simulation of Eq. (4) for diffusively unstable adiabatic flame ($\alpha=1.3$). Front configurations for $t/10=100$, 150, 200; $\mathbf{r}/10=(X,Y)$. Inset: a magnified segment of the last position of the front.

configurations in Fig. 2 are 1/10 of the real ones. The initially circular front develops a weak [in comparison with solutions of Eq. (3)] turbulent-cellular structure. The typical cell size as well as approximately circular general shape are sustained for all times and larger scales do not occur. One can observe a relatively small jump in the propagation velocity at the onset of the diffusive instability, which remains at the average new level without increasing any further.

III. EFFECTS DUE TO HEAT LOSSES

As was mentioned earlier the heat losses may dramatically enhance the impact of the diffusive instability leading to the flame self-fragmentation and formation of flame caps or balls. The latter as has been recently shown by Buckmaster, Joulin, and Ronney ([6,7]) may survive even beyond the planar flame quenching threshold.

For the moderately nonadiabatic flame the dispersion relation (2) is modified to (Joulin and Clavin [8], Sivashinsky and Matkowsky [9])

$$\sigma=D_{\rm th}\left[\frac{\alpha-1-2\ln\mu}{1+2\ln\mu}\right]k^2 -D_{\rm th}l_{\rm th}^2\left[\frac{4+2\ln\mu}{\mu^2(1+2\ln\mu)}\right]k^4\ , \tag{5}$$

where $U=\mu U_b$ is the speed of a planar nonadiabatic flame. The factor μ is determined by the relation

$$\nu=\mu^2\ln(1/\mu)\ , \tag{6}$$

where ν is the heat-loss intensity.

As one approaches the planar flame propagation limit ($\mu\to 1/\sqrt{e}$) the instability region expands. Simultaneously one observes a sharp increase in the instability rate σ.

In the vicinity of the quenching point the asymptotic relation (5) is clearly not valid and requires an appropriate modification. In particular, precisely at the quenching point the unstable branch of the pertinent dispersion relation reads (cf. Joulin and Clavin [8], Sivashinsky and Matkowsky [9], Joulin and Sivashinsky [10])

$$\sigma=\tfrac{1}{2}\gamma_{\rm eff}U_q|k|-D_{\rm th}k^2\ , \tag{7}$$

where $U_q=U_a/\sqrt{e}$ is the flame speed at the quenching point; $\gamma_{\rm eff}=\sqrt{4\alpha/\alpha+6}$. The analysis presented in Sivashinsky and Matkowsky [9] and Joulin and Sivashinsky [10] pertains to the limit of small α.

As is readily seen the latter relation is formally identical to that of hydrodynamic instability (1). Due to the functional similarity on the linear level one may try to extrapolate it on the nonlinear dynamics as well where hydrodynamic instability enjoys rather a well founded evolution equation (3). Hence, for the threshold flames, the following model equation is proposed:

$$\mathbf{n}\cdot\frac{d\mathbf{r}}{dt}=-U_q+D_{\rm th}\mathcal{K} +\frac{1}{2}\gamma_{\rm eff}U_q\left[1+\frac{1}{\pi}\int_S\frac{(\mathbf{r}-\mathbf{s})\cdot\mathbf{n}}{|\mathbf{r}-\mathbf{s}|^2}dS\right]\ . \tag{8}$$

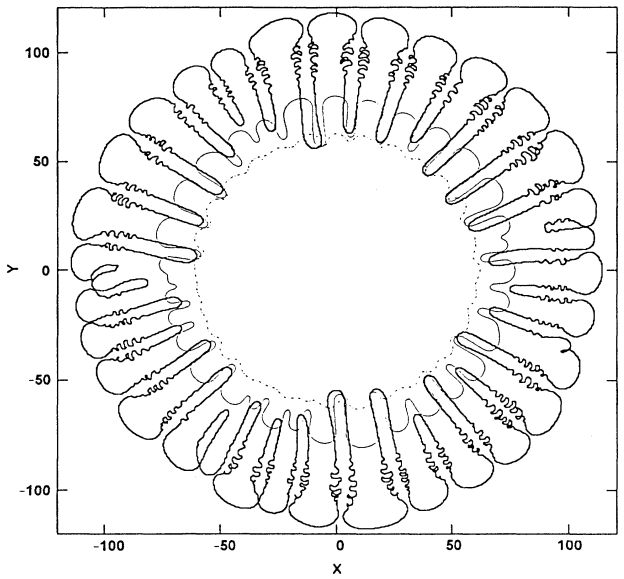

FIG. 3. Numerical simulation of Eq. (8) for a diffusively unstable flame at the quenching threshold ($\gamma_{\text{eff}}=1.5$). Front configurations for $t/3=60$ (dotted line), $t=67$ (thin line), and $t=74$; $\mathbf{r}/3=(X,Y)$.

We observe that while the thermal expansion parameter γ of Eq. (3) never exceeds unity, its counterpart γ_{eff} in Eq. (8) may come rather close to 2 provided the parameter $\alpha=\frac{1}{2}\beta(\text{Le}^{-1}-1)$ is large enough.

Numerical simulations of Eq. (8) presented in Fig. 3 (times and scales correspond to $\frac{1}{3}$ of the real ones), show that at $\gamma_{\text{eff}}>1$ the latter yields quite a plausible picture of the incipient stage of the flame self-fragmentation, which in its appearance resembles the so-called fingering instability typical for many other nonequilibrium systems involving interfaces. The bases of the fingers, once they are formed, remain close to their initial positions while the finger tips (cells) rapidly move forward. There is, however, some differences between the subsequent finger-tip evolution and the actual dynamics of the flame self-fragmentation.

According to the experimental observations the individual cells retaining fixed size move far apart from each other, finally turning into quite autonomous spherical or hemispherical flamelets (Ronney [3]). On the other hand, the finger tips produced by Eq. (8) gradually swell up, which eventually leads to the interface self-crossing. This discrepancy may apparently be attributed to the phenomenological nature of the model (8), which may well lack certain important features inherent to the real near-limit systems. A more systematic approach based on the unstable as well as stable branches of the pertinent dispersion relation, however, is likely to require a coupled set of equations both for the flame interface and its temperature (Joulin and Sivashinsky [10]).

IV. CONCLUDING REMARKS

Equation (8) corresponds to the planar flame quenching threshold and is, therefore, not applicable for the flame dynamics beyond this point where combustion may still survive in the form of corrugated or cap and ball-like structures. The pertinent weakly nonlinear model was proposed by Joulin and Sivashinsky [10]. Yet, our recent numerical simulations of the model showed that apart from the well behaved stable cellular configurations described by Joulin [11] and Sinay and Williams [12,13], under certain initial conditions one may well end up with a rapidly decelerating corrugated flame where effective speed backs off to minus infinity within a finite time interval. This outcome is likely to be just a reflection of the fingering character of the near limit instability whose uniform description requires involvement of the higher-order geometrical and perhaps reaction rate nonlinearities as well. A rational resolution of this issue will be attempted in a future work.

Models formulated in terms of the flame interface evolving in the physical space by their very nature are valid only up to the moment of the flame self-fragmentation. Beyond this point one is likely to obtain a self-crossing interface—a situation which should clearly be regarded as a mathematical artifact. To circumvent this difficulty one may try the scalar field, the so-called G equation, approach (Kerstein, Ashurst, and Williams [14]), which proved to be rather effective in the description of the flame fragmentation induced by the underlying vortical flows (Ashurst and Sivashinsky [15] and Aldredge [16]).

ACKNOWLEDGMENTS

These studies have been supported by the U.S. Department of Energy (Grant No. DE FG02-88ER13822), by the National Science Foundation (Grant No. CTS-9521084 and DMS-9305228), and by the U.S.-Israel Binational Science Foundation (Grant No. 93-00030).

[1] G. I. Sivashinsky, Ann. Rev. Fluid. Mech. **15**, 179 (1983).
[2] L. Filyand, G. I. Sivashinsky, and M. Frankel, Physica (Amsterdam) **72D**, 110 (1994).
[3] P. D. Ronney, Combust. Flame **62**, 121 (1990).
[4] M. L. Frankel, Phys. Fluids A **2**, 1979 (1990).
[5] (a) M. L. Frankel and G. I. Sivashinsky, J. Phys. (Paris) **48**, 25 (1987); (b) M. L. Frankel and G. I. Sivashinsky, Physica (Amsterdam) **30D**, 28 (1988).
[6] J. Buckmaster, G. Joulin, and P. Ronney, Combust. Flame **70**, 381 (1990).
[7] J. Buckmaster, G. Joulin, and P. Ronney, Combust. Flame **84**, 411 (1991).

[8] G. Joulin and P. Clavin, Combust. Flame **35**, 139 (1979).
[9] G. I. Sivashinsky and B. D. Matkowsky, SIAM J. Appl. Math. **40**, 255 (1981).
[10] G. Joulin and G. I. Sivashinsky, Combust. Sci. Tech. **31**, 75 (1983).
[11] G. Joulin, Combust. Sci. Tech. **47**, 69 (1986).
[12] L. Sinay and F. A. Williams, SIAM J. Appl. Math. **52**, 416 (1992).
[13] L. Sinay and F. A. Williams, in *Dynamics of Gaseous Combustion,* edited by A. L. Kuhl, J.-C. Leyer, A. A. Borisov, and W. A. Sirignano, Progress in Astronautics and Aeronautics Vol. 151 (AIAA, Washington, D.C., 1993), p. 263.
[14] A. R. Kerstein, Wm. T. Ashurst, and F. A. Williams, Phys. Rev. A **37**, 2728 (1988).
[15] Wm. T. Ashurst and G. I. Sivashinsky, Combust. Sci. Tech. **80**, 159 (1991).
[16] R. C. Aldredge (unpublished).
[17] M. L. Frankel (unpublished).